

An XMM-Newton and Chandra investigation of the nuclear accretion in the Sombrero Galaxy (NGC 4594)

S. Pellegrini

Astronomy Department, Bologna University, Italy

pellegrini@bo.astro.it

A. Baldi

G. Fabbiano

D.-W. Kim

Harvard-Smithsonian Center for Astrophysics, Cambridge, MA, USA

abaldi, pepi, kim@head-cfa.harvard.edu

ABSTRACT

We present an analysis of the XMM-Newton and Chandra ACIS-S observations of the LINER nucleus of the Sombrero galaxy and we discuss possible explanations for its very sub-Eddington luminosity by complementing the X-ray results with high angular resolution observations in other bands. The X-ray investigation shows a hard ($\Gamma = 1.89$) and moderately absorbed ($N_H = 1.8 \times 10^{21} \text{ cm}^{-2}$) nuclear source of $1.5 \times 10^{40} \text{ erg s}^{-1}$ in the 2–10 keV band, surrounded by hot gas at a temperature of $\sim 0.6 \text{ keV}$. The bolometric nuclear luminosity is at least ~ 200 times lower than expected if mass accreted on the supermassive black hole, that *HST* shows to reside at the center of this galaxy, at the rate predicted by the spherical and adiabatic Bondi accretion theory and with the high radiative efficiency of a standard accretion disc. The low luminosity, coupled to the observed absence of Fe-K emission in the nuclear spectrum, indicates that such a disc is not present. This nucleus differs from bright unobscured AGNs also for the lack of high flux variability and of prominent broad $H\alpha$ emission. However, it is also too faint for the predictions of simple radiatively inefficient accretion taking place at the Bondi rate; it could be too radio bright, instead, for radiatively inefficient accretion that includes strong mass outflows or convection. This

discrepancy could be solved by the possible presence of nuclear radio jets. An alternative explanation of the low luminosity, in place of radiative inefficiency, could be unsteady accretion.

Subject headings: galaxies: active – galaxies: individual (NGC4594) – galaxies: nuclei – X-rays: galaxies – X-rays: ISM

1. Introduction

Nearby galactic spheroids are believed to host supermassive black holes (SMBHs; e.g., Kormendy & Richstone 1995; Richstone et al. 1998). However, only low level LINER activity (Ho et al. 1997) or no sign of activity are almost the rule for these systems. This radiative quiescence represents one of the most intriguing aspects of SMBHs in the nearby Universe. The Sombrero galaxy (NGC 4594) is well known to host a SMBH at its nucleus, whose mass ($\sim 10^9 M_\odot$) has been established directly by *HST* measurements (Kormendy et al. 1996). The nucleus of Sombrero is also a LINER 2 (Heckman 1980; Ho et al. 1997), a compact and variable radio continuum source (e.g. Hummel et al. 1984; Bajaja et al. 1988) and a pointlike source in an *HST* high resolution image (Crane et al. 1993). Thanks to its proximity (d=9.4 Mpc, Ajhar et al. 1997) and the availability of high angular resolution observations, this nucleus represents an ideal case to study in detail how the modality of accretion changes from high luminosity to low luminosity AGNs. The answer to this question is key to the knowledge of the history of accretion in the Universe (e.g., Haiman et al. 2003).

Sombrero was first detected in X-rays with *Einstein*. Although its X-ray luminosity was included in a list of LINERs (Halpern & Steiner 1983), subsequent more detailed work showed an extended source (see Forman et al. 1985; Fabbiano et al. 1992). A ROSAT HRI image detected a luminous, possibly variable, pointlike source associated with the nucleus (Fabbiano & Juda 1997), with a (0.1–2.4) keV luminosity of $\sim 9 \times 10^{39}$ erg s⁻¹ (when rescaled for the distance adopted here). ASCA and BeppoSAX spectra suggest the presence of a moderately absorbed power law (of photon index $\Gamma \sim 1.9$), as well as a softer thermal component of $kT \sim 0.6$ keV (Nicholson et al. 1998; Terashima et al. 2002; Pellegrini et al. 2002). An upper limit of 150 eV and 260 eV was placed on the equivalent width of an Fe-K line at 6.4 keV and 6.7 keV respectively. A *Chandra* snapshot exposure showed an image dominated by the nucleus (Ho et al. 2001) whose spectrum again was found consistent with a moderately absorbed hard power law (Pellegrini et al. 2002).

Comparison of the X-ray, H α and radio emission of the nuclear source with those of bright AGNs suggests that it may be a low luminosity version of the latter (Fabbiano & Juda

1997; Pellegrini et al. 2002). However, the shape of the whole spectral energy distribution of this nucleus compares well with those of other low luminosity AGNs (Ho 1999), all of which reveal the absence of a big blue bump.

If the nuclear X-ray emission is due to accretion onto the SMBH, its luminosity is extremely sub-Eddington ($L(2 - 10 \text{ keV}) \sim 10^{-7} L_{Edd}$, Pellegrini et al. 2002). This fact, coupled to the absence of an Fe-K detection, suggest that this nucleus may be a good test case for radiatively inefficient accretion (Rees et al. 1982; Narayan & Yi 1995). It is also interesting to compare this nucleus to other recently studied sub-Eddington nuclei of “normal” elliptical galaxies, such as IC 1459 (Fabbiano et al. 2003) and NGC1399, NGC4636, NGC4472 (Loewenstein et al. 2001).

We report here a study of the nucleus of the Sombrero galaxy based on deep XMM and *Chandra* observations. XMM’s excellent sensitivity at both soft and hard X-rays allows us to measure accurately the hard power law component and set stringent limits on the Fe-K emission. The high resolution archival *Chandra* ACIS-S observation allows us to study the circumnuclear region and constrain the amount of fuel available to feed the nucleus. With both results we obtain a more complete picture of the physical state of this X-ray faint LINER nucleus.

2. Observations and Data preparation

Table 1 summarizes the observing log. The Sombrero galaxy was observed by XMM-*Newton* during revolution 376 (PI: Fabbiano; ObsID 0084030101) on December 28, 2001 for a total exposure time of 40 ks, and with *Chandra* ACIS-S (PI: Murray; ObsID 1586) on May 31, 2001 for a total of 18.7 ks.

The XMM-*Newton* data were processed using the Science Analysis Software (*XMM-SAS*) v5.3. The event files were ‘cleaned’ of background flares, caused by soft (< a few 100 keV) protons hitting the detector surface. These flares were found analyzing the light curves at energies greater than 10 keV (in order to avoid contribution from real X-ray source variability) and setting a threshold for good time intervals at 0.35 cts/s for each *MOS* unit and at 0.55 cts/s for the *pn* unit. Soft proton flares removal and a duration of the observation of about half the scheduled exposure time resulted in a substantial reduction of the useful integration time in the *pn*, for which we obtained 17 ks. For the *MOS1* and the *MOS2* instead we obtained 34.6 ks and 40.5 ks, respectively.

We used the archival *Chandra* observation in conjunction with the XMM-*Newton* data to derive information on the nuclear surroundings on the small scale. The *Chandra* data

were processed using CIAO v2.3 data analysis software.

3. Spectral analysis of the XMM nuclear data

An EPIC XMM-*Newton* view of the Sombrero galaxy is shown in Figure 1. The image shows a prominent pointlike nuclear source surrounded by diffuse emission and several off-nuclear pointlike sources (most likely luminous galaxian X-ray binaries).

To investigate the spatial properties of the nuclear emission, we have compared the radial profile of the nuclear source with the EPIC point response function (PSF; Figure 2) normalized to the detected counts in the central $1''$ bin around the nucleus. The radial profile agrees well with the PSF out to a radius of $\sim 7 - 8''$. At larger radii, the contribution of non-nuclear emission becomes important. Given the presence of both pointlike and extended emission, we have performed spectral analyses on the counts extracted from two circles of different radii ($20''$ and $7''$) centered on the nucleus, and compared the results to assess the uncertainty on the spectral parameters of the nuclear source resulting from galaxian contamination. The $20''$ radius corresponds to ~ 0.9 kpc at the distance of the galaxy and to an encircled energy fraction (EEF) of 0.75; the $7''$ radius corresponds to a physical size of ~ 0.3 kpc and to an EEF of 0.42. In both cases, the background was extracted from a source free circular region outside the optical galaxy having a radius of 80 arcsec. We used both EPIC *MOS* and *pn* data, coadding *MOS1* and *MOS2* spectra, to optimize the signal-to-noise ratio of the data. The latest versions of the response matrices (v6.2) were used for the fit. The spectra were rebinned in order to have at least 20 counts for each energy bin and we used XSPEC for the spectral analysis. We fitted together the *MOS* and *pn* data, leaving their relative normalization free to vary.

Tables 2 and 3 summarize the results of the spectral analysis. All the errors are quoted at 90% for two interesting parameters. We used two different models: a simple absorbed power law model (XSPEC model: $wabs(zwabs(pow))$), where *wabs* is fixed at the Galactic absorbing column of $N_H = 3.7 \times 10^{20} \text{ cm}^{-2}$, (Stark et al. 1992)) and a composite power law plus thermal model ($wabs(mekal + zwabs(pow))$), with abundance fixed at 0.5 solar), in order to model the emission from a possible extended circumnuclear hot interstellar medium.

The simple power law fit gives a χ^2 of 556.9 with 527 degrees of freedom (corresponding to a probability of 17.8%) for the $20''$ data, and a χ^2 of 330.2 with 320 degrees of freedom (probability of 33.6%) for the $7''$ data. The best fit photon index is the same within the errors for the two spectra ($\Gamma = 1.89 \pm 0.03$ and $\Gamma = 1.88_{-0.04}^{+0.05}$ respectively). It is consistent with that obtained from BeppoSAX data and is somewhat higher than, although still marginally

consistent with, that found from a spectral analysis of the nucleus with the snapshot ACIS-S exposure (Pellegrini et al. 2002). The intrinsic absorbing column density is only moderate; it increases for the smaller extraction radius [going from (1.3 ± 0.1) to $(1.8 \pm 0.1) \times 10^{21}$ cm^{-2}], which suggests contamination by a soft possibly thermal component outside the 7'' radius. The N_H from the 7'' data is consistent with that from the analysis of the snapshot ACIS-S exposure and marginally higher than the BeppoSAX value, which can easily be due to the difference in the extraction radius.

The power law + thermal model fit gives a better representation of the 20'' spectrum, with a χ^2 of 537.3 for 525 degrees of freedom (probability of 34.6%). An F-test demonstrates that this improvement is significant (F-test significance $\sim 10^{-4}$). We find no improvement instead for the 7'' spectrum, where we obtain a χ^2 of 326 for 318 degrees of freedom (probability of 36.6%). In both cases, the intrinsic N_H and the photon index are consistent with those obtained from the simple power law fit. The best fit temperature of the thermal component is $kT = 0.61$ keV. Not surprisingly, the 20'' fit returns a larger value for the luminosity of this component. The 20'' and 7'' spectra, their modelings and fit residuals, and the confidence contours for the intrinsic N_H , kT and Γ are shown in Figure 3 and 4.

Adding to the absorbed power law model an iron $K\alpha$ emission line at 6.4 keV, for the 7'' spectrum, does not improve the fit. We can set an upper limit on the equivalent width (EW) of this line of 145 eV, for a narrow line, and of 296 eV for a broad Gaussian line with line width $\sigma = 0.43$ keV (as found on average for Seyfert 1's by Nandra et al. (1997b)).

We have not used the 18.7 ks exposure ACIS-S data for the spectral analysis of the nucleus because they are strongly affected by pile-up.

4. Mass accretion rate

While pileup makes the interpretation of *Chandra* data ambiguous for the nuclear source, thanks to the very sharp *Chandra* PSF these data provide unique information on the circum-nuclear region, as near as 2'' from the nucleus, corresponding to < 100 pc at the distance of Sombrero. Figure 5 shows a view of the central regions of this galaxy resulting from the 18.7 ks ACIS-S exposure; the image has been obtained with adaptive smoothing, i.e., after applying a tool that smoothes a two-dimensional image with a circular Gaussian kernel of varying size (here, from 1 to 20 pixels; see <http://cxc.harvard.edu/ciao/ahelp/csmooth.html>).

The high resolution ACIS-S data allow us to derive the density and temperature profile of the interstellar matter in the surroundings of the nuclear SMBH by using a deprojection technique implemented within XSPEC. Spectra extracted from three elliptical annuli

centered on the nucleus were compared with the spectra expected from the superposition along the line of sight of the emission coming from the corresponding ellipsoidal shells. The elliptical annuli have a major/minor axis ratio of 1.5, equal to that of the Sombrero’s bulge. To avoid contamination from the nucleus, we chose as inner boundary of the first annulus a 2'' circle; its outer boundary is an ellipse with semiminor axis of 3''.33 and semimajor axis of 5''. The outer boundary of the second annulus has a semiminor axis of 6'' and a semimajor axis of 9''. The third annulus has as outer boundary an ellipse with semiminor axis of 10''.67 and a semimajor axis of 16''. From these annuli we subtracted clearly visible point sources. Assuming that the emission comes from hot gas plus residual contamination from unresolved binaries (see, e.g., Kim & Fabbiano 2003), we obtained deprojected density and temperature profiles by fitting together the spectra of the 3 annuli with the XSPEC model *project*wabs(raymond+powerlaw)*. The power law index was fixed at $\Gamma = 1.9$, *wabs* was fixed at the Galactic value and the temperature and normalizations were free parameters. The resulting temperature and density profiles are shown in Figure 6.

The above calculation was next used to derive an estimate of the mass supply rate for accretion on the SMBH, by applying the Bondi (1952) theory of steady, spherical and adiabatic accretion. This requires T and n at “infinity”, in practice near the accretion radius (that in the case of Sombrero is $r_A = GM_{BH}/c_s^2 \sim 30$ pc, with c_s the sound speed). The inner radius of the innermost annulus (~ 90 pc) is a factor of ~ 3 larger than r_A . Moreover, the temperature and density profiles show a sharp positive gradient toward smaller radii. Therefore, in order to have an estimate of the Bondi mass accretion rate (\dot{M}_{Bondi}), an extrapolation of the kT and n values at r_A is required. Since the uncertainties on these values are large (Fig. 6), we derived for \dot{M}_{Bondi} the maximum range allowed by the uncertainties, via a linear extrapolation of the outer T, n data that also considers their errorbars. From the formula

$$\dot{M}_{Bondi} = 6.2 \times 10^{23} M_9^2 T_{0.8}^{-3/2} n_{0.15} g s^{-1}$$

where M_9 is the SMBH mass in units of $10^9 M_\odot$ (for Sombrero $M_{BH} \simeq 10^9 M_\odot$, Kormendy et al. 1996), $T_{0.8}$ is the temperature in units of 0.8 keV and $n_{0.15}$ is the density in units of 0.15 cm^{-3} [see, e.g., eq. (3) of Di Matteo et al. (2003)], we found that $\dot{M}_{Bondi, min} \simeq 0.008 M_\odot \text{ yr}^{-1}$ and $\dot{M}_{Bondi, max} \simeq 0.067 M_\odot \text{ yr}^{-1}$. The best fit temperature and density values of the innermost annulus ($kT = 0.65$ keV; $n = 0.15 \text{ cm}^{-3}$) give $\dot{M}_{Bondi} \simeq 0.013 M_\odot \text{ yr}^{-1}$.

5. Discussion

We discuss here possible scenarios to explain the very sub-Eddington luminosity of the Sombrero’s nucleus, using the results of our analysis of high quality X-ray data and

information coming from high angular resolution observations in other bands.

5.1. Heavily obscured emission?

The bolometric luminosity of the Sombrero’s nucleus is $L_{bol} \sim 2.5 \times 10^{41}$ erg s⁻¹ [obtained by integrating the spectral energy distribution (SED) in Fig. 7], that is $2 \times 10^{-6} L_{Edd}$. This very sub-Eddington nuclear luminosity could be explained by Compton thick material surrounding the nucleus and heavily absorbing the X-ray emission, as in Seyfert 2 galaxies. However, as observed in similar nuclei (e.g., IC 1459, Fabbiano et al. 2003), though not with the high XMM’s sensitivity that we can exploit here, the spectral characteristics of the emission are not consistent with this picture. There is no sign of heavy obscuration and the small amount of absorption needed for modeling the spectrum could be explained by intervening dust: an *HST* V–I image shows a dusty nuclear environment (Pogge et al. 2000), for which Emsellem & Ferruit (2000) derive $A_V=0.5$ mag (that corresponds to an intrinsic $N_H = 8.3 \times 10^{20}$ cm⁻², for the Galactic extinction law). Moreover, the upper limit on the equivalent width of Fe-K emission at 6.4 keV (EW < 145 eV, Sect. 3) rules out the presence of a strong 6.4 keV iron fluorescence line, of $EW \gtrsim 1$ keV, that is expected in the Compton thick scenario (as in NGC1068; e.g., Matt et al. 1997). Absence of high extinction is also supported by the *HST* FOS spectra in the UV band (Nicholson et al. 1998; Maoz et al. 1998).

5.2. Downsized AGN?

This nucleus shows some similarities with the observed emission properties of luminous AGNs: an X-ray/radio luminosity ratio comparable with the extrapolation of the bright radio galaxy correlation (Fabbiano et al. 1984); a spectral power law consistent with that of Seyfert 1 galaxies (Nandra et al. 1997a); 2–10 keV and $H\alpha$ luminosities consistent with the low luminosity extension of the $L_X - L_{H\alpha}$ correlation found for powerful Seyfert 1 nuclei and quasars (Ward et al. 1988; Ho et al. 2001).

However, its bolometric luminosity is well below what we would expect from efficient accretion of the available fuel. The SMBH is surrounded by hot gas whose density and temperature can be measured close to the accretion radius. If at very small radius this gas joins an accretion disc with a standard radiative efficiency $\eta \sim 0.1$, as in brighter AGNs, it should produce a luminosity:

$$L_{acc} = \eta \dot{M}_{Bondi} c^2 \simeq (4.5 - 38) \times 10^{43} \text{ erg s}^{-1}$$

for the range of \dot{M}_{Bondi} at the accretion radius estimated in Sect. 4. This is at least ~ 200 times higher than the observed L_{bol} , which represents a strong argument against a thin disc in this nucleus. An additional argument could be that its SED (Fig. 7) lacks the ‘blue bump’ (UV/blue excess) observed in luminous AGNs and attributed to the accretion disc (Shields 1978). This lack is a feature common to other low luminosity AGNs (Ho 1999). However, the spectral energy distribution of a multicolor black body accretion disc (e.g., Frank et al. 1992), with a mass accretion rate in the range estimated in Sect. 4 for \dot{M}_{Bondi} and $M_{BH} = 10^9 M_{\odot}$, shows a peak at a frequency of $\sim (1.8 - 3.0) \times 10^{14}$ Hz, which is redder than in the B and U bands.

Besides the very low luminosity, inconsistent with efficient disc accretion, there are other properties in which the Sombrero’s nucleus differs from Seyfert 1’s nuclei: (1) the latter exhibit iron K emission lines produced in the accretion disc, whose strength clearly increases with decreasing X-ray luminosity; the average EW of the 6.4 keV emission (for a broad Gaussian fit) is ~ 300 eV at an X-ray luminosity of $\text{few} \times 10^{42}$ erg s $^{-1}$ (Nandra et al. 1997b), while our analysis gives an upper limit of $\text{EW} < 296$ eV at a much lower luminosity (Sect. 3). (2) Seyferts show evidence for X-ray flux variability, with the amplitude anticorrelated with the source luminosity (Nandra et al. 1997a). Neither short term nor long term variability has been detected in or between our and previous X-ray observations of the Sombrero’s nucleus (Fabbiano & Juda 1997; Pellegrini et al. 2002; Terashima et al. 2002). In the 18ks ACIS-S data we have looked for variability to take full advantage of the unprecedented angular resolution. The pileup does not affect the temporal variation (as we expect a constant fraction of X-rays migrating from low energies to higher energies). We have applied a traditional time-binned histogram analysis and a Bayesian block technique for unbinned data, which was developed for the *Chandra* Multi-wavelength Project (Kim et al. 2003). In both tests we do not find any statistically significant variability. The XMM flux ($F(2 - 10 \text{ keV}) = 1.3 \times 10^{-12}$ erg s $^{-1}$ cm $^{-2}$) is also consistent with that given by the *Chandra* snapshot data ($F(2 - 10 \text{ keV}) = 1.6 \times 10^{-12}$ erg s $^{-1}$ cm $^{-2}$, Pellegrini et al. 2002). The somewhat larger flux estimated from the ASCA and BeppoSAX data is entirely consistent with the much larger aperture used in these cases. (3) Finally, the small N_H derived from the XMM data is inconsistent with the absence of prominent broad line emission (Panessa & Bassani 2002), which contrasts with the predictions of the unification models of bright Seyfert nuclei (Antonucci 1993).

5.3. Radiatively inefficient accretion?

An alternative possibility is that accretion proceeds at a rate not far from \dot{M}_{Bondi} but with a low radiative efficiency, through an advection dominated optically thin quasi spherical hot accretion flow (ADAF; e.g., Narayan & Yi 1995). In these models, unlike in the standard, radiatively efficient, thin disc models, very little of the gravitational potential energy of the inflowing gas is radiated away and accretion lacks the cold, optically thick gas required for the emission of the fluorescent 6.4 keV Fe-K line. The majority of the observable emission is in the X-ray and in the radio bands. In the X-rays it comes from thermal bremsstrahlung with a flat power law ($\Gamma < 1.5$ in the *Chandra* band) or inverse Compton scattering of soft synchrotron photons by the flow electrons, with a steeper X-ray spectral shape (e.g., $\Gamma \sim 2.2$ has been used to model the nucleus of M87, Di Matteo et al. 2003). In the radio band, synchrotron emission arises from the strong magnetic field in the inner parts of the accretion flow.

Detailed ADAF modeling has been applied many times to low luminosity AGNs and normal ellipticals (e.g., Quataert et al. 1999; Di Matteo et al. 2001; Loewenstein et al. 2001). The absence of a fluorescent Fe line from cold material and the observed X-ray photon index of the Sombrero’s nucleus are in accordance with the ADAF predictions. Also, the radio emission from an ADAF scales with the SMBH mass and the X-ray luminosity as $L_{15\text{ GHz}} \sim 10^{36} (M_{BH}/10^7 M_{\odot}) (L_{2-10\text{ keV}}/10^{40} \text{ erg s}^{-1})^{0.14} \text{ erg s}^{-1}$ (Yi & Boughn 1999). This relation gives a predicted $L_{15\text{ GHz}} \sim 1.06 \times 10^{38} \text{ erg s}^{-1}$ for Sombrero. VLBI measurements (Hummel et al. 1984) reveal a flat spectrum core source with $L_{15\text{ GHz}} = 1.58 \times 10^{38} \text{ erg s}^{-1}$, therefore the radio-to-X-rays ratio agrees with the predictions of the basic ADAF. However, an ADAF modeling tailored to the Sombrero’ nucleus, and using a range of $\dot{M}_{Bondi} = 0.01 - 0.1 M_{\odot} \text{ yr}^{-1}$ that includes the range found here, showed that the ADAF synchrotron emission overestimates significantly (by as much as a factor of ~ 10) the observed radio flux (Di Matteo et al. 2001).

More recent work on radiatively inefficient accretion has revealed that little mass available at large radii is actually accreted on the SMBH and most of it is lost to an outflow or circulates in convective motions (Blandford & Begelman 1999; Stone et al. 1999; Igumenshchev et al. 2003). If the density is lower in the inner flow regions, the synchrotron emission in the radio band is drastically reduced. In the case of Sombrero, strong mass loss with only a few percent of \dot{M}_{Bondi} actually accreted on the SMBH helps reconcile the model with the observations *in the radio* band (Di Matteo et al. 2001). However, in these models the radio-to-X-rays ratio changes with respect to the ‘basic’ ADAF predictions, in the sense that outflows or convection suppress the radio emission more than the X-ray one (Quataert & Narayan 1999). Therefore, if these models are normalized to match the observed X-ray

luminosity of the Sombrero’s nucleus, they will exhibit a deficit of radio emission with respect to the observations. In this picture, an additional radio source (e.g., a nuclear jet) could solve the discrepancy. The presence of jets was suggested by Di Matteo et al. (2001), who in fact best reproduced the flat radio spectral shape of the Sombrero’s nucleus with self-absorbed synchrotron emission originating from a compact region (while the ADAF synchrotron radiation has an inverted spectrum up to high radio frequencies, above which it abruptly drops).

In conclusion, even in the case of low radiative efficiency the mass accretion rate on the SMBH must be less than \dot{M}_{Bondi} to match the observed emission level. Note that the *Chandra* upper limits on the X-ray nuclear luminosities of three ellipticals also require strong outflows or convection in an ADAF (Loewenstein et al. 2001); and this could be the case also for the nucleus of M32 (Ho et al. 2003). Note finally that a few other low luminosity AGNs exhibit an excess of radio emission relative to the predictions of low radiative efficiency models (see Quataert et al. 1999; Ulvestad & Ho 2001; Di Matteo et al. 2001).

5.4. Jet dominated emission?

Recent radio observations show that a strong jet presence is a common feature of LINERs (Nagar et al. 2001) and recent modeling of low luminosity AGNs (Falcke & Biermann 1999; Yuan et al. 2002) suggests that the higher wavelengths may also be dominated by the jet emission. In this modeling the accretion flow can be described either by a standard Shakura-Sunyaev disc or an ADAF, and a fraction of the accretion flow is advected into a jet, which represents an important component of the emission spectrum (actually dominating in low luminosity sources). In fact, Livio et al. (1999) have argued that the Blandford & Znajek (1977) mechanism might be most relevant for advection dominated flows.

In these models the synchrotron emission from the base of the jet produces a “bump” of emission from radio to high IR frequencies, peaking roughly at mid-IR. The flat/inverted radio synchrotron spectrum comes from further out in the jet. Its optically thin part, plus self-Comptonized emission and external Compton emission from the jet, produce the X-ray spectrum. A flat radio spectrum (Hummel et al. 1984) and a peak in the IR region are features shown by the SED of the Sombrero’s nucleus (Fig. 7). Moreover, such a jet dominated model has been applied recently to explain the whole spectral energy distribution of the LINER in the elliptical galaxy IC1459 (Fabbiano et al. 2003). Similarly to the Sombrero’s nucleus, the X-ray emission of IC1459 is modeled with an unabsorbed power law of $\Gamma = 1.88 \pm 0.09$ (using the *Chandra* ACIS-S data).

It is interesting to note that in this modeling the jets are by far the dominant sink of power, in the form of kinetic and internal energy, to the point that $\sim 0.1L_{acc}$ could be stored in them. A similar fraction was estimated for the jet power in the case of the FRI galaxy IC4296, using again ACIS-S data to estimate L_{acc} plus a direct calculation of the jet kinetic power, instead of a modeling of the SED (Pellegrini et al. 2003).

5.5. Low mass supply?

Alternatively to the possibilities described in the previous section, the mass supply to the central SMBH could be much lower than estimated in Sect. 4, because accretion is not an adiabatic process and perhaps it is not even steady. This is the case of feedback modulated accretion models where the interstellar medium is heated by the energy input from a central source that decreases or stops recursively the accretion on the central SMBH, giving raise to cycles of activity. Such a scenario has been argued several times over the last decade: the ISM could be heated by the impact of collimated outflows (Tabor & Binney 1993; Binney 1999; Kaiser & Binney 2003; Di Matteo et al. 2001, 2003) or by inverse Compton scattering of hard photons (Ciotti & Ostriker 2001), both coming from the central nucleus. Therefore, accretion is only episodic, and between phases of accretion activity is switched off with a low nuclear luminosity. In the Ciotti & Ostriker (2001) scenario, at the present time the duty cycle of activity includes short bright phases followed by prolonged periods of re-”adjustment” of the gas surrounding the nucleus, so that only $1/10^4$ to $1/10^3$ nuclei in the nearby Universe should be caught in the bright AGN phase.

Signatures of the central heating include disturbances in the X-ray isophotes of the gas. In Sombrero, the X-ray isophotes in the circumnuclear region shown by the ACIS-S image (Fig. 5) do not reveal clear disturbances from nuclear outflows/hard photons heating the ISM with respect to a round distribution. However, this aspect is difficult to assess given the crowding of stellar sources close to the center and it is under study. The same holds for the possible presence of temperature variations in the circumnuclear region.

We just note three observational facts that certainly contrast with the predictions of a global “cooling flow” in this bulge: a) the hot gas temperature shows an increase close to the center, instead of a smoothly decreasing profile (Fig. 6), even though the errors are large to establish firmly that central heating is occurring; b) the mass accretion rate \dot{M}_{Bondi} , although derived for a steady and adiabatic case that may not apply, is already much less than the stellar mass loss rate \dot{M}_* in this bulge [$\dot{M}_* \sim 0.36 M_\odot \text{ yr}^{-1}$ from the prescriptions of the stellar evolution theory, e.g., inserting the bulge luminosity $L_B = 2.4 \times 10^{10} L_\odot$ (Ho et al. 1997) in eq. (3) of Ciotti et al. 1991]; c) the ratio L_X/L_B for the diffuse emission in the

bulge ($L_X = 9 \times 10^{39}$ erg s⁻¹ from Fabbiano & Juda (1997)) is far too low for the hot gas to be in a global inflow (Ciotti et al. 1991; Fabbiano et al. 1992). Points a,b,c are instead consistent with a nuclear induced global degassing of the bulge, as predicted for low mass systems by the Ciotti & Ostriker (2001) heating scenario. A detailed analysis and modeling of the status of the hot gas on the galactic scale is in progress.

6. Conclusions

By exploiting XMM’s sensitivity and *Chandra*’s high angular resolution we have studied the X-ray properties of the nucleus of the Sombrero galaxy. We have then examined various possibilities for the observed low level of activity shown by this well known LINER, and these can be summarized as follows:

- The presence of heavy obscuration is ruled out by the observed properties of the X-ray spectrum.
- The nuclear bolometric luminosity is at least ~ 200 times lower than expected if the central SMBH accreted matter at the rate predicted by the steady, spherical and adiabatic Bondi accretion theory, with the high radiative efficiency of a standard accretion disc. Therefore, the final stages of accretion are not radiatively efficient and/or the mass supply on the SMBH is far less.
- In a radiatively inefficient accretion scenario, where the rate of accreting mass is close to the Bondi estimate, the model luminosity is higher than observed. Including outflows or convection can fix this problem, but then, if the observed X-ray emission is accounted for, the radio luminosity is underreproduced. It could then come from nuclear jets.
- A jet dominated emission model, recently applied to a few other low luminosity AGNs, could perhaps explain the observed spectral energy distribution. If this model applies, a large fraction of the accretion luminosity L_{acc} could be stored in the form of jet power.
- Another possibility is that accretion is not steady and adiabatic, therefore the Bondi theory does not apply. That is, due to the presence of a central heating source, far less mass than predicted by the Bondi accretion rate actually reaches the SMBH. Observed signatures of a central heating could be an increase in the temperature profile close to the nucleus and a low hot gas content for the bulge.
- In addition to the absence of a standard accretion disc, other important differences with the properties of luminous type 1 AGNs include the lack of flux variability and Fe-K emission. Also, this LINER 2 shows no strong absorption therefore the orientation dependent

unified scheme devised for bright AGNs does not apply to it.

We thank A. Zezas for help with the data analysis and discussions. This work was supported under the NASA XMM GO program (PI G. Fabbiano), and the Chandra X-ray Center contract (NAS 8-39073). S.P. acknowledges funding from ASI (ASI contracts IR/037/01 and IR/063/02) and MURST.

REFERENCES

- Antonucci, R., 1993, *ARA&A*, 31, 473
- Bajaja, E., Hummel, E., Wielebinski, R., Dettmar, R. J. 1988, *A&A*, 202, 35
- Binney, J., 1999, proceedings of a workshop held at Ringberg Castle, Tegernsee, Germany, 15-19 September 1997; Hermann-Josef Röser, Klaus Meisenheimer, eds. Berlin; New York: Springer, 1999. Lecture notes in physics, 530, p.116
- Blandford, R. D., Begelman, M. C. 1999, *MNRAS*, 303, L1
- Blandford, R.D., Znajek, R.L., 1977, *MNRAS*, 179, 433
- Bondi, H. 1952, *MNRAS*, 112, 195
- Ciotti, L., D’Ercole, A., Pellegrini, S., Renzini, A. 1991, *ApJ*, 376, 380
- Ciotti, L., Ostriker, J. P. 2001, *ApJ*, 551, 131
- Crane, P., et al. 1993, *AJ*, 106, 1371
- Di Matteo, T., Carilli, C. L., Fabian, A. C. 2001, *ApJ*, 547, 731
- Di Matteo, T., Allen, S. W., Fabian, A. C., Wilson, A. S., Young, A. J. 2003, *ApJ*, 582, 133
- Emsellem, E., Ferruit, P. 2000, *A&A*, 357, 111
- Fabbiano, G., Trinchieri, G., Elvis, M., Miller, L., Longair, M. 1984, *ApJ*, 277, 115
- Fabbiano, G., Kim, D. W., Trinchieri, G. 1992, *ApJS*, 80, 531
- Fabbiano, G., Juda, J. Z. 1997, *ApJ*, 476, 666
- Fabbiano, G., Elvis, M., Markoff, S., Siemiginowska, A., Pellegrini, S., Zezas, A., Nicastro, F., Trinchieri, G., McDowell, J., 2003, *ApJ*, 588, 175

- Falcke, H., Biermann, P. L. 1999, A&A, 342, 49
- Forman, W., Jones, C., Tucker, W. 1985, ApJ, 293, 102
- Frank, J., King, A., Raine, D., 1992, *Accretion Power in Astrophysics*, Cambridge University Press.
- Haiman, Z., Ciotti, L., Ostriker, J. P., ApJ-submitted, astro-ph/0304129
- Halpern, J. P., Steiner, J. E. 1983, ApJ, 269, L37
- Heckman, T. M. 1980, A&A, 87, 152
- Ho, L. C., Filippenko, A. V., Sargent, W. L. W. 1997, ApJ, 487, 568
- Ho, L. C. 1999, ApJ, 516, 672
- Ho, L. C., et al. 2001, ApJ, 549, L51
- Ho, L. C., Terashima, Y., Ulvestad J.S. 2003, ApJ589, 783
- Hummel, E., van der Hulst, J. M., Dickey, J. M 1984, A&A, 134, 207
- Igumenshchev I.V., Narayan R., abramowicz M.A. 2003, ApJ, in press
- Kaiser, C. R., Binney, J. 2003, MNRAS, 338, 837
- Kim, D. W., Fabbiano, G. 2003, ApJ, 586, 826
- Kim, D. W., et al. 2003, submitted to ApJS
- Kormendy, J., Richstone, D. 1995, ARA&A, 33, 581
- Kormendy, J., et al. 1996, ApJ, 473, L91
- Livio M., Ogilvie G. I., & Pringle J. E. 1999, ApJ, 512, 100
- Loewenstein, M., Mushotzky, R. F., Angelini, L., Arnaud, K. A., Quataert, E. 2001, ApJ, 555, L21
- Maoz, D., Koratkar, A., Shields, J.C., Ho, L.C., Filippenko, A.V., Sternberg, A. 1998, ApJ, 116, 55
- Matt, G., et al. 1997, A&A, 325, L13
- Nagar, N. M., Wilson, A. S., Falcke, H. 2001, ApJ, 559, L87

- Nandra, K., George, I. M., Mushotzky, R. F., Turner, T. J., Yaqoob, T. 1997a, ApJ, 476, 70
- Nandra, K., George, I. M., Mushotzky, R. F., Turner, T. J., Yaqoob, T. 1997b, ApJ, 477, 602
- Narayan, R., Yi, I. 1995, ApJ, 452, 710
- Nicholson, K.L., Reichert, G.A., Mason, K.O., et al. 1998, MNRAS, 300, 893
- Panessa, F., Bassani, L. 2002, A&A, 394, 435
- Pellegrini, S., Fabbiano, G., Fiore, F., Trinchieri, G., Antonelli, A. 2002, A&A, 383, 1
- Pellegrini, S., Venturi, T., Comastri, A., Fabbiano, G., Fiore, F., Vignali, C., Morganti, R., Trinchieri, G. 2003, ApJ, 585, 677
- Pogge, R. W., Maoz, D., Ho, L. C., Eracleous, M. 2000, ApJ, 532, 323
- Quataert, E., di Matteo, T., Narayan, R., Ho, L. C. 1999, ApJ, 525, L89
- Quataert, E., Narayan, R. 1999, ApJ,
- Rees, M. J., Phinney, E. S., Begelman, M. C., Blandford, R. D. 1982, Nature, 295, 17
- Richstone, D., et al. 1998, Nature, 395, 14
- Shields, G. A. 1978, Nature, 272, 706
- Stark A.A., Gammie C.F., Wilson R.W., Bally J., Linke R.A., Heiles C. & Hurwitz M., 1992, ApJS, 79, 77
- Stone, J.M., Pringle, J.E., Begelman, M.C., 1999, MNRAS, 310, 1002
- Tabor, G., Binney, J. 1993, MNRAS, 263, 323
- Terashima, Y., Iyomoto, N., Ho, L. C., Ptak, A. F. 2002, ApJS, 139, 1
- Ulvestad, J.S., Ho, L.C. 2001, ApJ, 562, L133
- Ward, M. J., Done, C., Fabian, A. C., Tennant, A. F., Shafer, R. A. 1988, ApJ, 324, 767
- Yi, I., Boughn, S. P. 1999, ApJ, 515, 576
- Yuan, F., Markoff, S., Falcke, H., Biermann, P. L. 2002, A&A, 391, 139

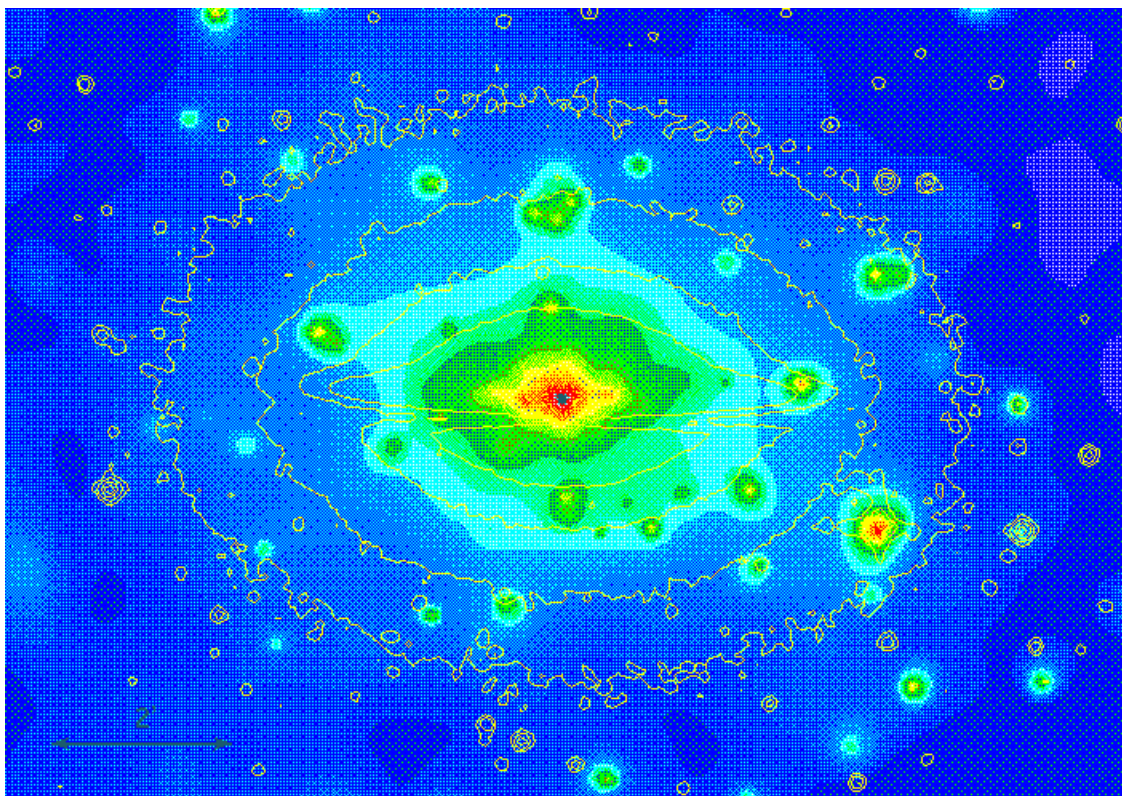


Fig. 1.— Adaptively smoothed XMM-*Newton* EPIC image of the Sombrero galaxy (0.5-2 keV band) with superimposed optical contours from the DSS. North is up and East to the left.

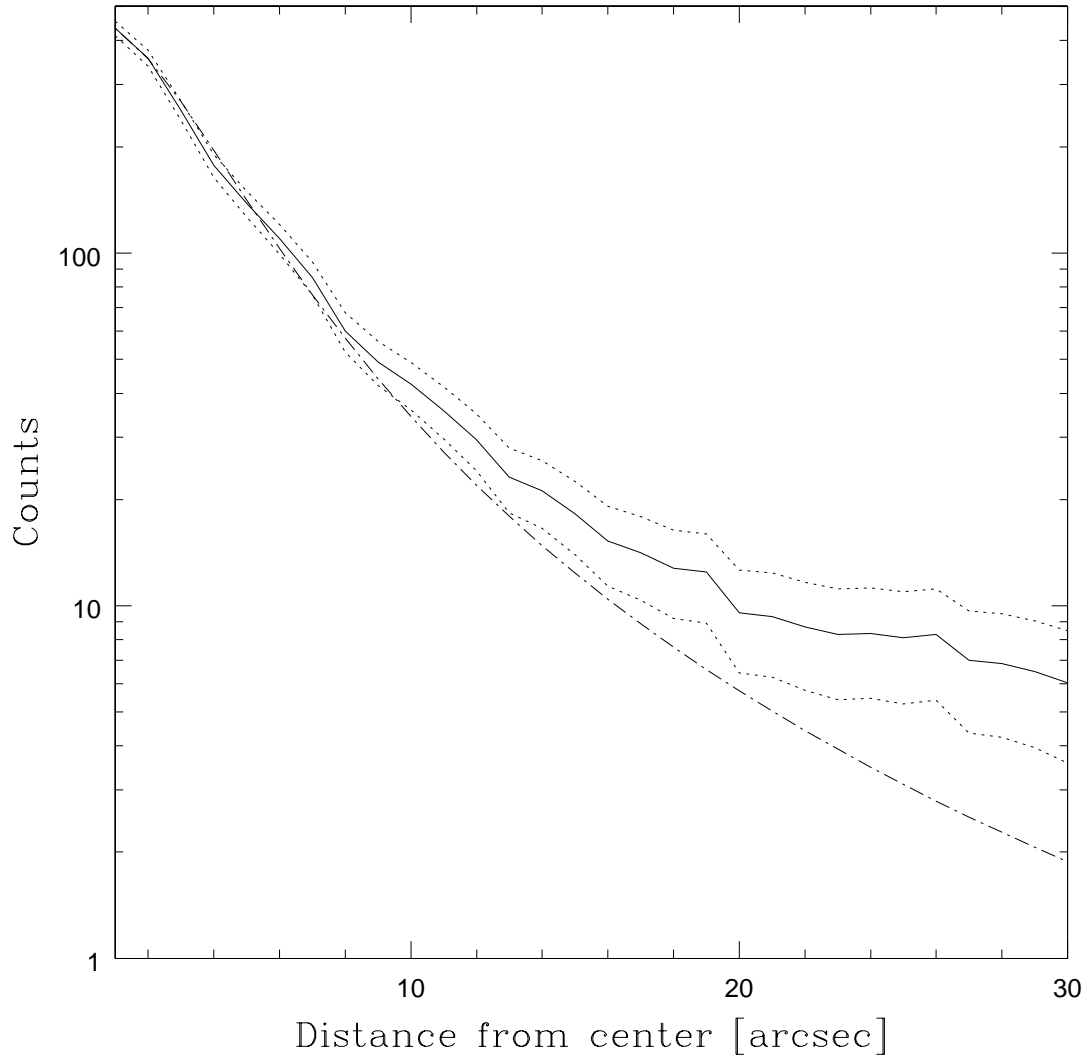


Fig. 2.— 0.5-2 keV band radial profile of the nucleus of Sombrero in EPIC MOS1 instrument compared with the instrumental PSF (dash-dotted line). The solid line represents the measured counts while dotted lines are the errors on the counts.

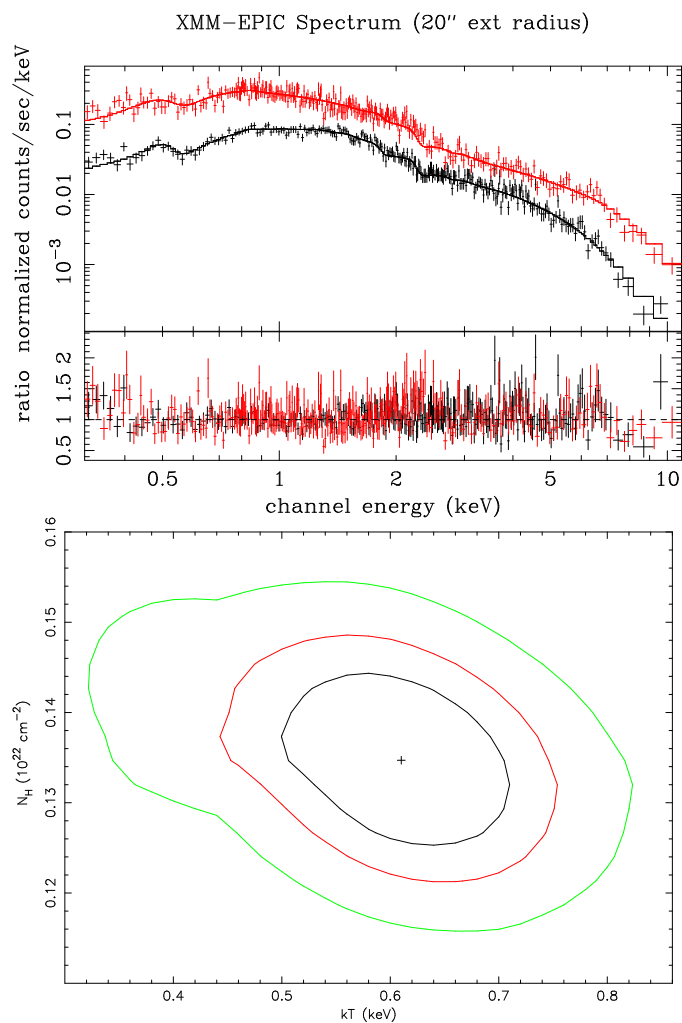


Fig. 3.— *Upper panel*: Sombrero nuclear EPIC MOS (black) and pn (red) spectra and fit residuals for an absorbed power law model plus thermal component, obtained from a 20 arcsec extraction radius. *Lower panel*: Confidence contours at 68%, 90% and 99% for the best-fit temperature kT and intrinsic absorbing column density N_H .

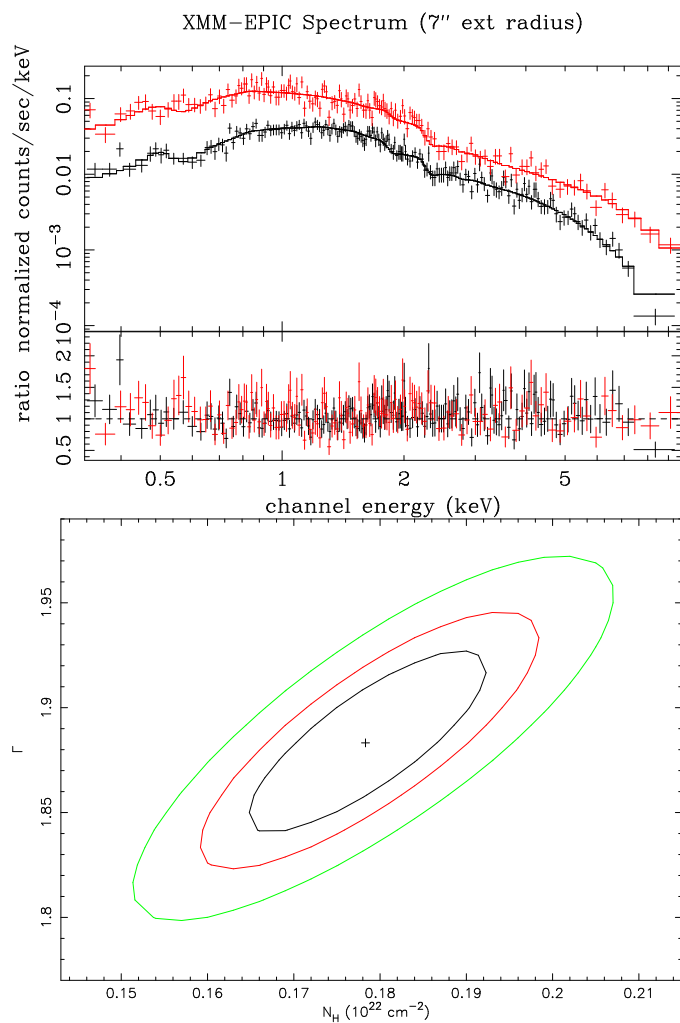


Fig. 4.— *Upper panel:* Sombrero nuclear EPIC MOS (black) and pn (red) spectra and fit residuals for a simple absorbed power law model, obtained from a 7 arcsec extraction radius. *Lower panel:* Confidence contours at 68%, 90% and 99% for the best-fit intrinsic absorbing column density N_H and photon index Γ .

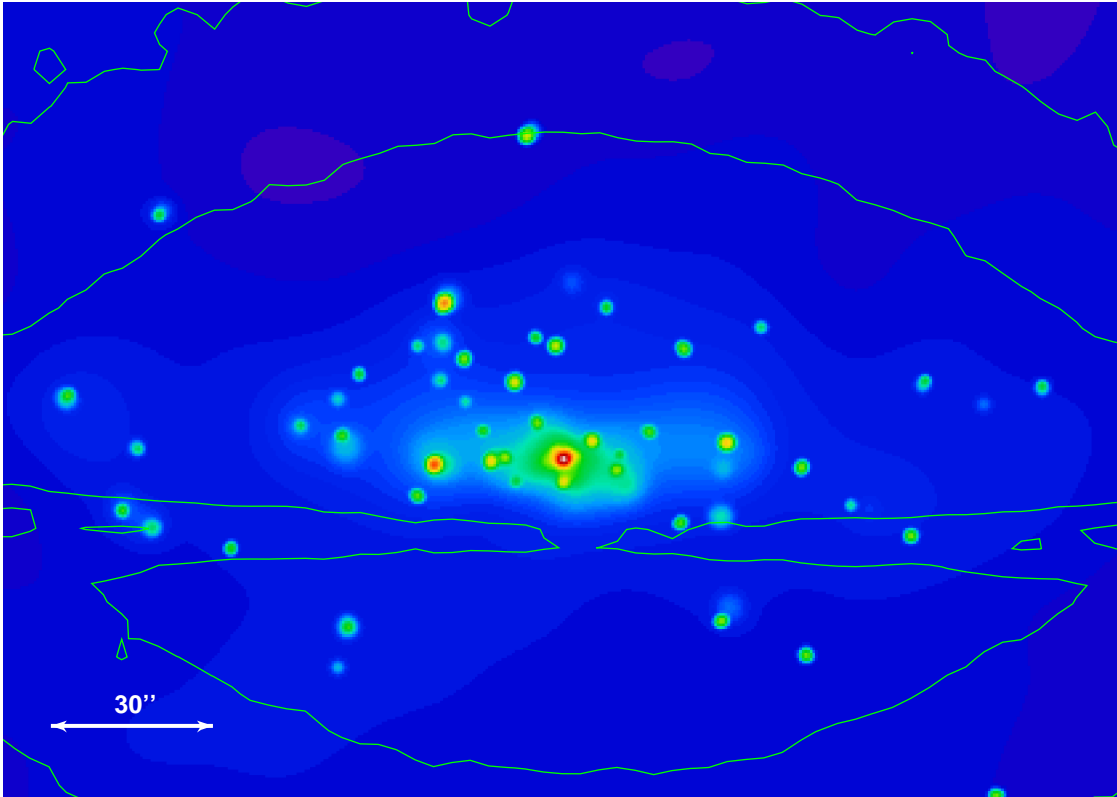


Fig. 5.— Adaptively smoothed *Chandra* ACIS-S image (0.3-10 keV band) of the Sombrero galaxy with superimposed optical contours from the DSS. North is up and East to the left.

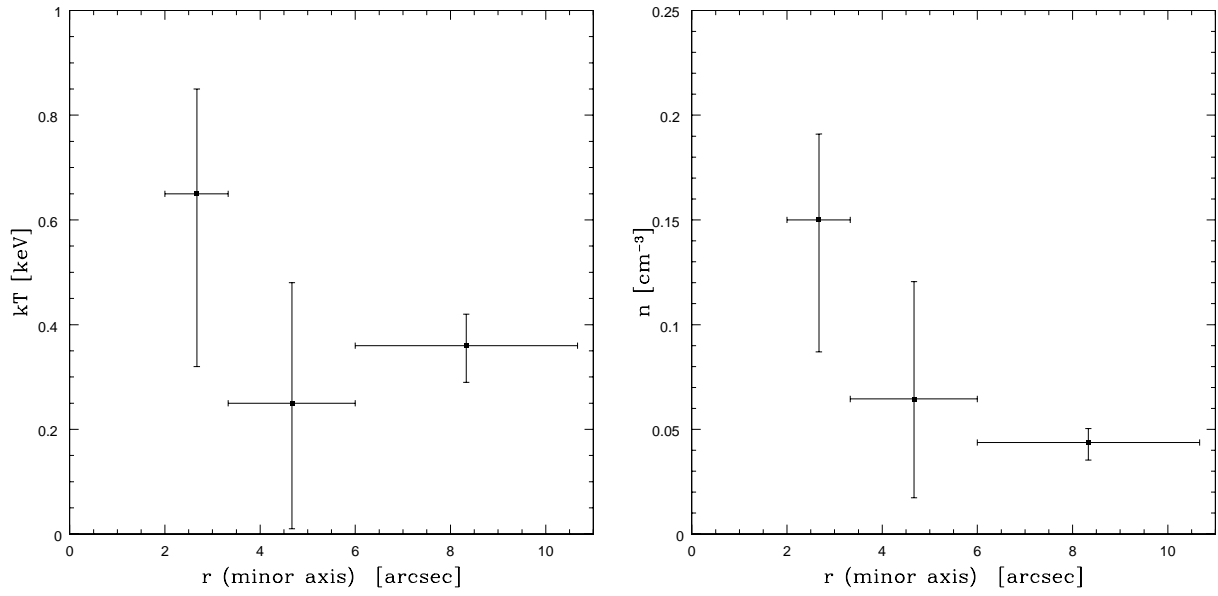


Fig. 6.— Temperature profile (left panel) and density profile (right panel) for the Sombrero galaxy. Errorbars indicate the 90% confidence interval.

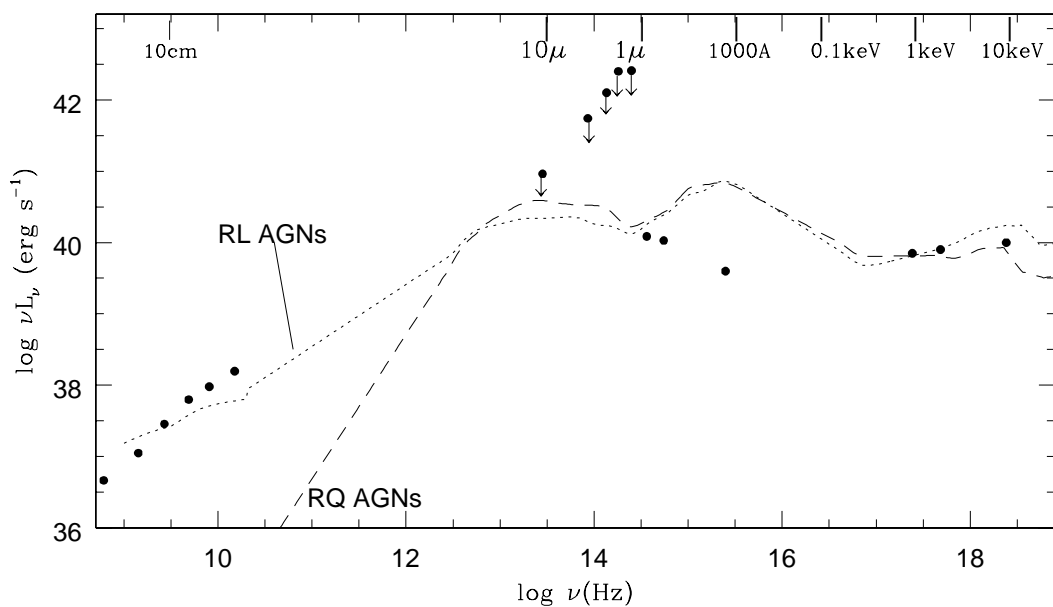


Fig. 7.— The spectral energy distribution of the nucleus of Sombrero from radio to X-rays. Radio data with subarcsecond resolution are from Hummel et al. 1984, IR data with $5''$ resolution (plotted as upper limits) are from Willner et al. 1985, optical and UV data with subarcsecond resolution are from the *HST* WFPC2 images and FOS spectrum (Ho 1999), the X-ray data are from this paper. Lines show the median distribution observed for low redshift radio quiet and radio loud AGNs (Elvis et al. 1994), renormalized to match the X-ray data.

Table 1. XMM-*Newton* EPIC and *Chandra* ACIS observation log

Instrument	Obs ID	Date	Filter/Grating	Performed duration (ks)
EPIC MOS1	0084030101	December 28, 2001	Thin	42.90
EPIC MOS2	0084030101	December 28, 2001	Thin	42.90
EPIC pn	0084030101	December 28, 2001	Thin	18.80
ACIS-S	1586	May 31, 2001	None	18.75

Table 2. Results of the EPIC XMM-*Newton* spectral analysis of the Sombrero nucleus: absorbed power law model. Fluxes are observed and corrected for the EEF, luminosities are intrinsic.

	20'' extraction radius	7'' extraction radius
χ^2/dof	556.9/527	330.2/320
Intrinsic N_H (cm^{-2})	$1.3 \pm 0.1 \times 10^{21}$	$1.8 \pm 0.1 \times 10^{21}$
Photon Index	1.89 ± 0.03	$1.88^{+0.05}_{-0.04}$
0.5-2 keV flux ($\text{erg cm}^{-2} \text{ s}^{-1}$)	$6.4 \pm 0.3 \times 10^{-13}$	$5.5^{+0.4}_{-0.3} \times 10^{-13}$
2-10 keV flux ($\text{erg cm}^{-2} \text{ s}^{-1}$)	$1.3 \pm 0.1 \times 10^{-12}$	$1.3 \pm 0.1 \times 10^{-12}$
0.5-2 keV luminosity (erg s^{-1})	$6.8 \pm 0.3 \times 10^{39}$	$5.7 \pm 0.4 \times 10^{39}$
2-10 keV luminosity (erg s^{-1})	$1.5 \pm 0.1 \times 10^{40}$	$1.4 \pm 0.1 \times 10^{40}$

Table 3. Results of the EPIC XMM-*Newton* spectral analysis of the Sombrero nucleus: absorbed power law plus thermal model. Fluxes are observed and corrected for the EEF, luminosities are intrinsic.

	20'' extraction radius	7'' extraction radius
χ^2/dof	537.3/525	326/318
kT (keV)	$0.61^{+0.11}_{-0.12}$	$0.67^{+0.27}_{-0.21}$
Intrinsic N_H (cm^{-2})	$1.4 \pm 0.1 \times 10^{21}$	$1.9^{+0.1}_{-0.2} \times 10^{21}$
Photon Index	1.86 ± 0.03	$1.89^{+0.02}_{-0.07}$
0.5-2 keV flux ($\text{erg cm}^{-2} \text{ s}^{-1}$) (power law)	$6.0 \pm 0.3 \times 10^{-13}$	$5.2 \pm 0.4 \times 10^{-13}$
0.5-2 keV flux ($\text{erg cm}^{-2} \text{ s}^{-1}$) (thermal comp.)	$2.6^{+0.9}_{-0.8} \times 10^{-14}$	$8.8 \pm 8.8 \times 10^{-15}$
0.5-2 keV luminosity (erg s^{-1}) (power law)	$6.4 \pm 0.3 \times 10^{39}$	$5.5 \pm 0.4 \times 10^{39}$
0.5-2 keV luminosity (erg s^{-1}) (thermal comp.)	$2.7^{+1.0}_{-0.9} \times 10^{38}$	$9.3 \pm 9.3 \times 10^{37}$